Supplementary Information

Transition Metal-Phenanthroline Intercalated Montmorillonite as Efficient Electrocatalysts for the Oxygen Evolution Reaction

*In Seon Lee,[†] Jae Ryeol Jeong,[†] Cu Dang Van, and Min Hyung Lee**

Department of Applied Chemistry, Kyung Hee University, Yongin, Gyeonggi 17104, Korea.

[†]These authors contributed equally to this work.

[*]**Corresponding Author:** minhlee@khu.ac.kr

Table S1. FT-IR vibrational frequencies of functional groups in Na-MMT, MMT:M(Phen)$_2$ composites, and 1,10-phenanthroline.

Sample	O-H	O-H	C-N	Si-O	Si-O-Al	Si-O
Na-MMT	3455	1636		1046	526	468
MMT:Ni(Phen)$_2$	3440	1636	1384	1047	525	468
MMT:Co(Phen)$_2$	3440	1624	1384	1047	526	468
MMT:Fe(Phen)$_2$	3440	1634	1384	1046	525	471
1, 10-Phenanthroline	3404		1345			

Table S2. X-ray diffraction analysis of basal spacing and interlayer heights of Na-MMT, MMT:Phen, and MMT:M(Phen)$_2$ composites.

Sample	Band Position (2θ)	Basal spacing (Å)	Interlayer (Å)
Na-MMT	6.88	12.8	3.2
MMT:Phen	4.77	18.5	8.9
MMT:Ni(Phen)$_2$	5.13	17.2	7.6
MMT:Co(Phen)$_2$	5.20	17.0	7.4
MMT:Fe(Phen)$_2$	5.25	16.8	7.2

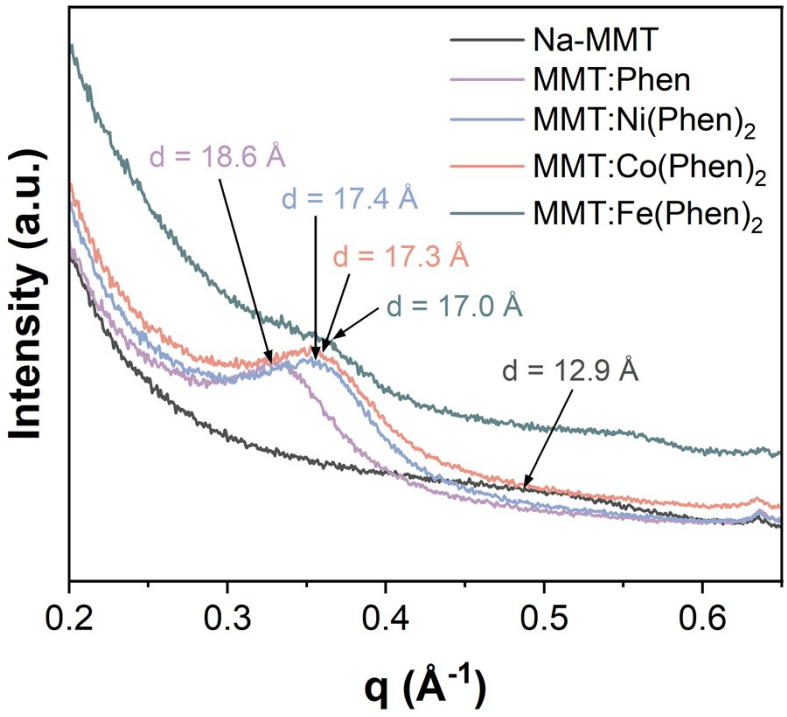

Figure S1. Small-angle X-ray scattering (SAXS) spectra of Na-MMT, MMT:Phen, and MMT:M(Phen)$_2$ composites.

Table S3. Small-angle X-ray scattering (SAXS) analysis of basal spacing and q-values of Na-MMT, MMT:Phen, and MMT:M(Phen)$_2$ composites.

Sample	q-value (Å^{-1})	Basal spacing (Å)
Na-MMT	0.488	12.9
MMT:Phen	0.337	18.6
MMT:Ni(Phen)$_2$	0.361	17.4
MMT:Co(Phen)$_2$	0.362	17.3
MMT:Fe(Phen)$_2$	0.369	17.0

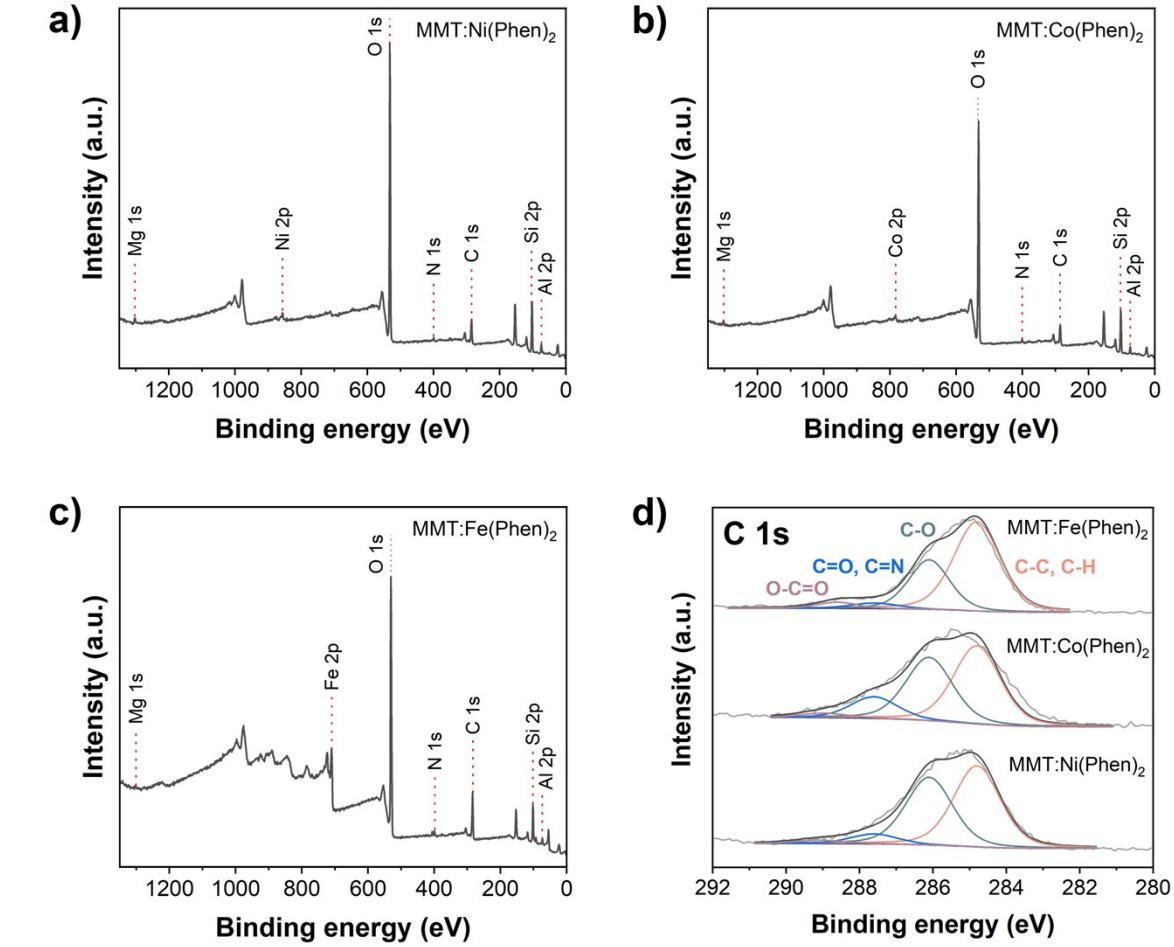

Figure S2. (a-c) XPS survey spectra and (d) high-resolution C 1s XPS spectra of MMT:M(Phen)$_2$ composites.

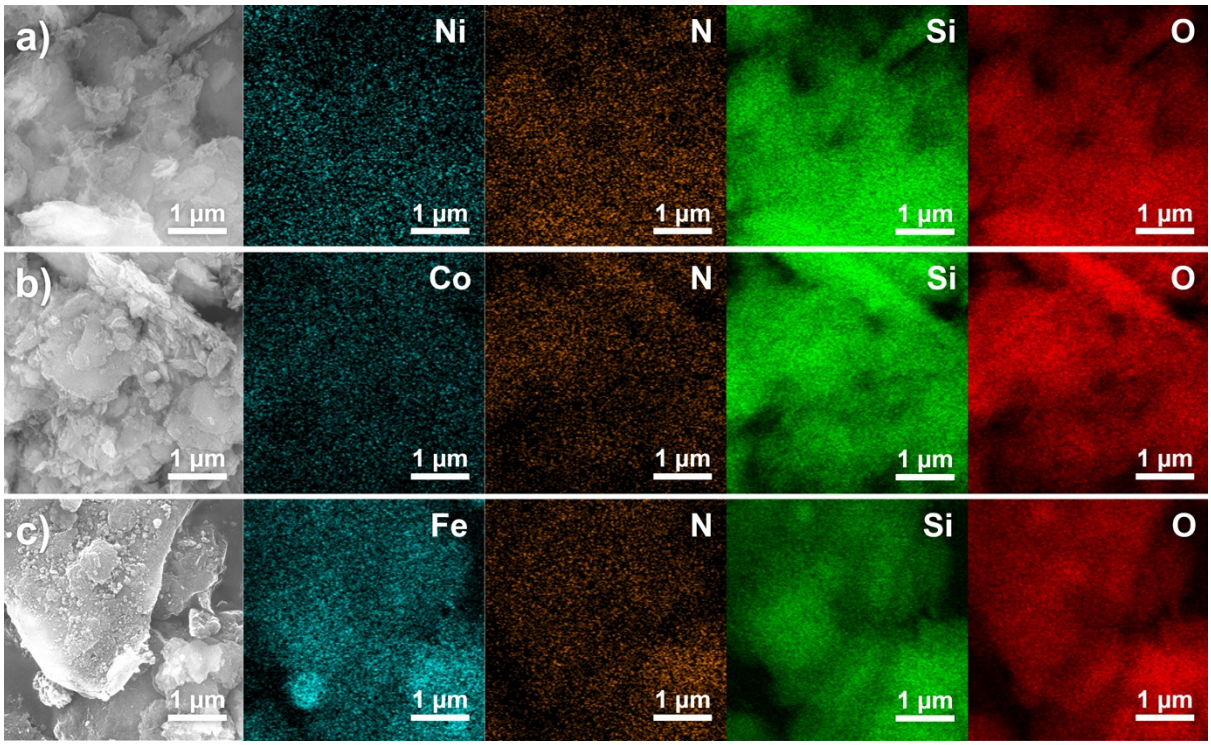

Figure S3. SEM images and energy-dispersive X-ray spectroscopy (EDS) analysis of (a) MMT:Ni(Phen)$_2$, (b) MMT:Co(Phen)$_2$, and (c) MMT:Fe(Phen)$_2$.

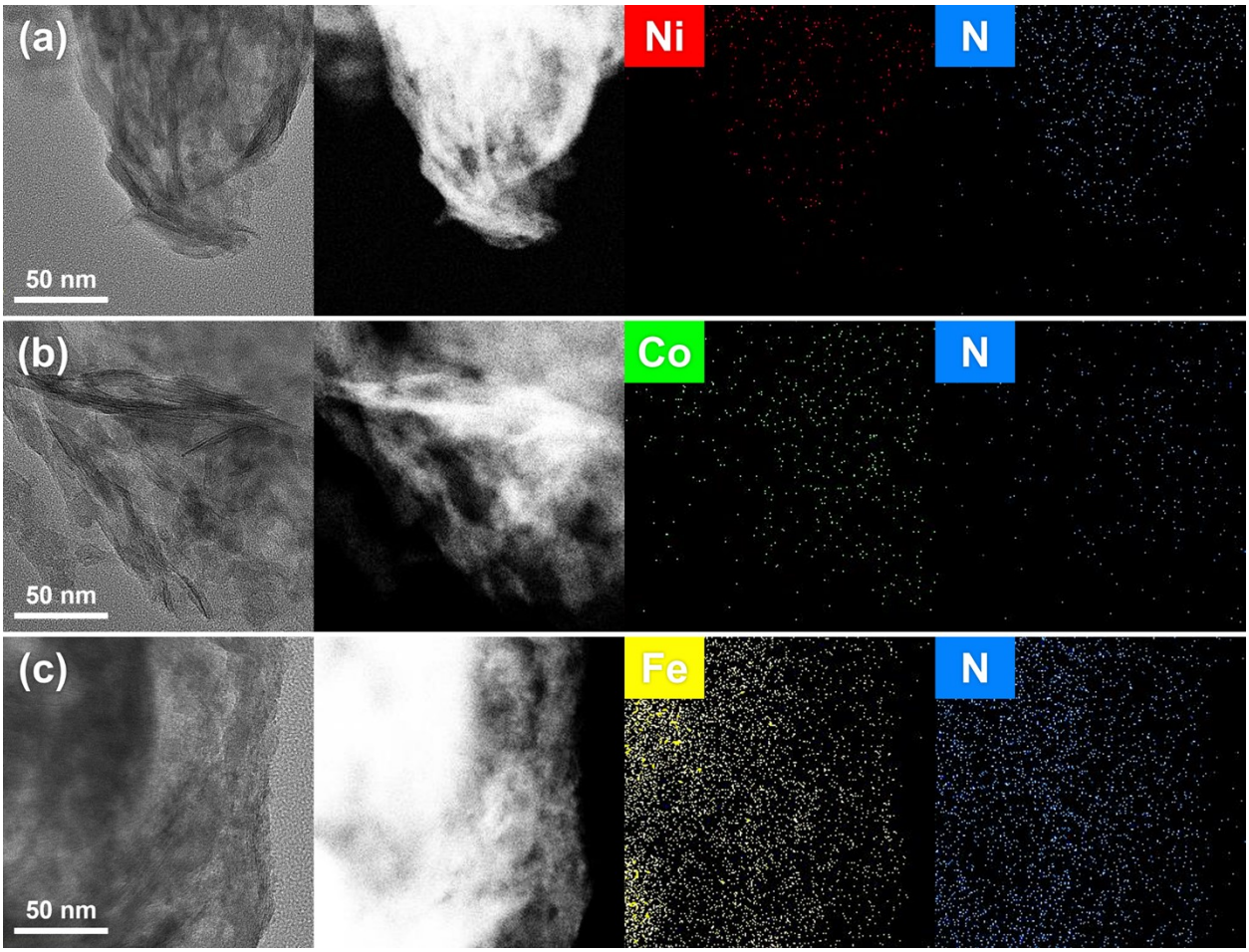

Figure S4. Cs-TEM images and energy-dispersive X-ray spectroscopy (EDS) analysis of (a) MMT:Ni(Phen)$_2$, (b) MMT:Co(Phen)$_2$, and (c) MMT:Fe(Phen)$_2$.

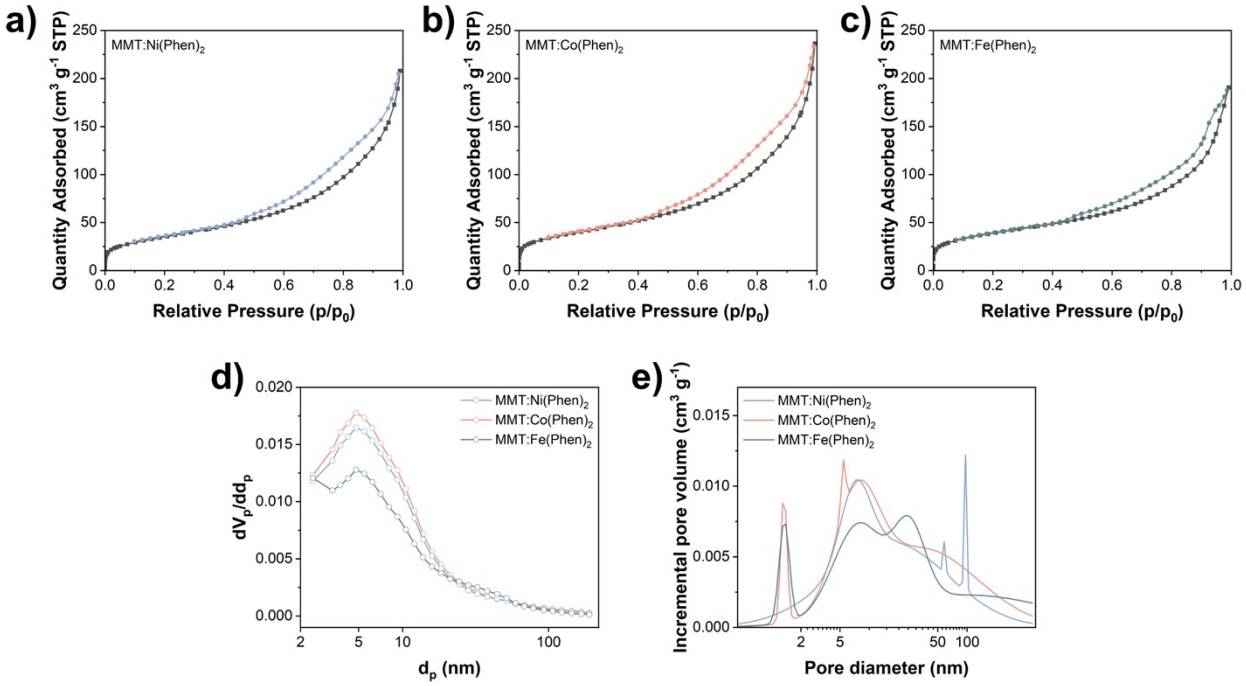

Figure S5. (a–c) Nitrogen adsorption/desorption isotherms at 77K for MMT:M(Phen)$_2$. (d) Barrett-Joyner-Halenda (BJH) pore size distribution; (e) Nonlocal density functional theory (NLDFT) pore size distribution of MMT:M(Phen)$_2$ composites.

Table S4. Physical properties of MMT:M(Phen)$_2$ composites determined from N_2 adsorption via BET analysis.

Sample	S_{BET} ($m^2 \cdot g^{-1}$)	S_{mes} ($m^2 \cdot g^{-1}$)	V_{mes} ($cm^3 \cdot g^{-1}$)	V_{tot} ($cm^3 \cdot g^{-1}$)
MMT:Ni(Phen)$_2$	124.71	123.77	0.2727	0.3204
MMT:Co(Phen)$_2$	139.95	132.21	0.2888	0.3509
MMT:Fe(Phen)$_2$	137.61	104.94	0.2474	0.2932

S_{BET}: The specific surface area; S_{mes}: The mesopore surface area; V_{mes}: The mesopore volume; V_{tot}: The total pore volume

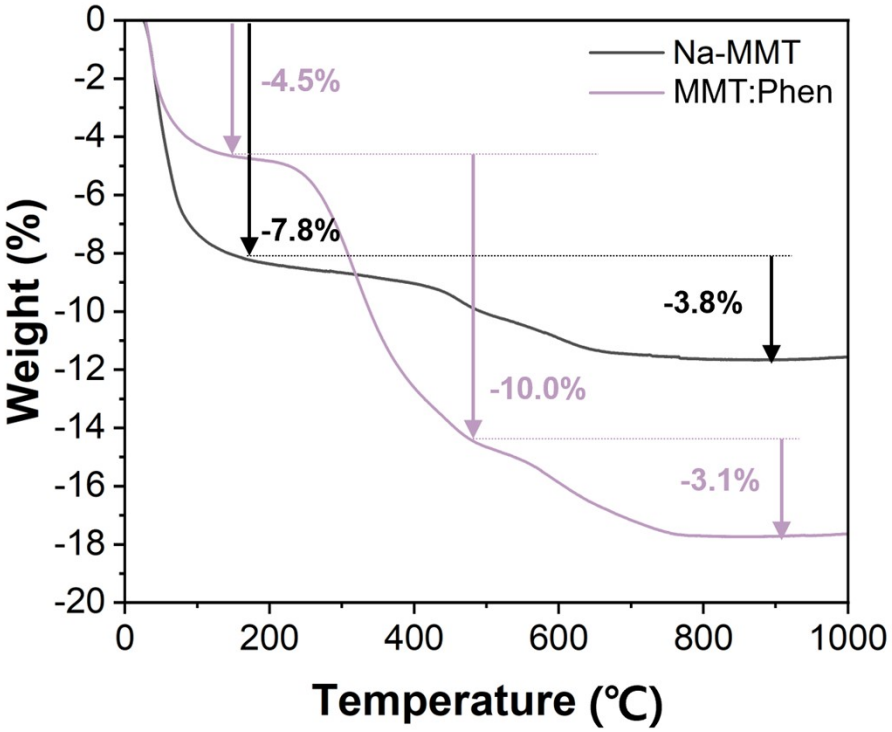

Figure S6. TGA curves depicting degradation patterns of Na-MMT and MMT:Phen.

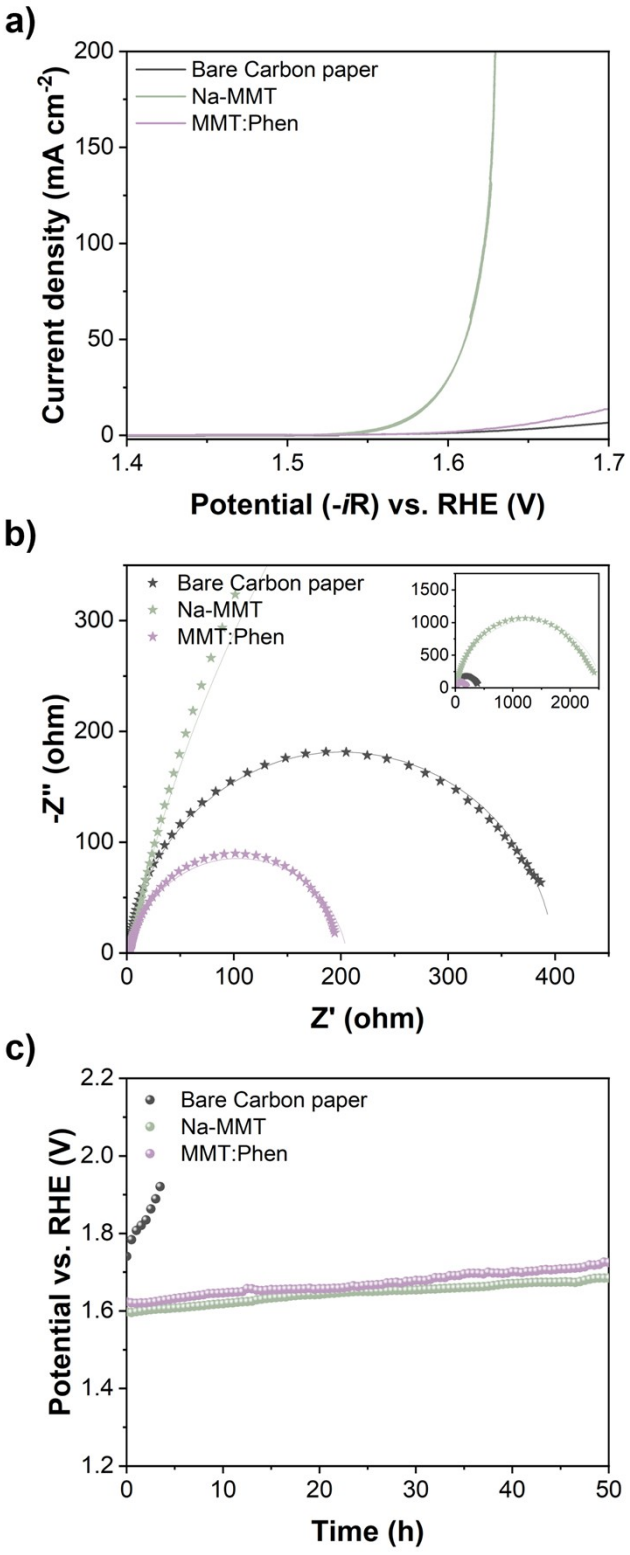

Figure S7. Electrochemical OER performance of catalysts. (a) linear sweep voltammetry (LSV) curves, (b) Nyquist plots, and (c) long-term stability tests at 10 mA·cm^{-2}.

Table S5. Comparative analysis of overpotential and charge transfer resistance (R_{ct}) of catalysts for OER.

Sample	Overpotential @ 10 mA·cm^{-2}	R_{ct}
Bare carbon paper	508 mV	274.1 Ω·cm^2
Na-MMT	347 mV	1858.6 Ω·cm^2
MMT:Phen	448 mV	167.3 Ω·cm^2
MMT:Ni(Phen)$_2$	320 mV	13.5 Ω·cm^2
MMT:Co(Phen)$_2$	313 mV	22.1 Ω·cm^2
MMT:Fe(Phen)$_2$	361 mV	1450.4 Ω·cm^2

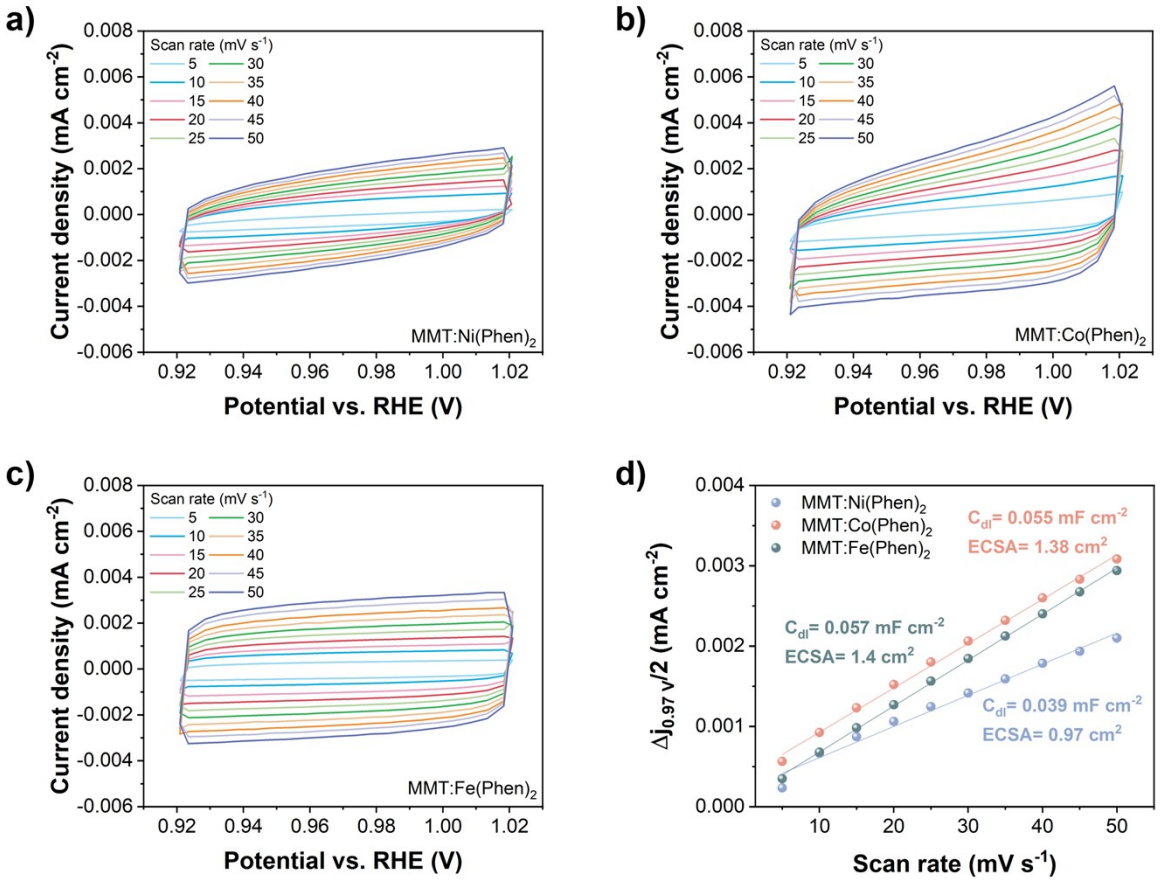

Figure S8. CV curves of catalysts (a) MMT:Ni(Phen)$_2$, (b) MMT:Co(Phen)$_2$, and (c) MMT:Fe(Phen)$_2$, and (d) the corresponding calculated double-layer capacitance (C_{dl}) values.

Table S6. Elemental concentrations in MMT composites based on ICP-MS analysis.

Sample	Element	Concentration (ppm = $mg \cdot kg^{-1}$)
Na-MMT	Ni	4.75
	Co	1.15
	Fe	1.53×10^4
MMT:Ni(Phen)$_2$	Ni	1.6×10^4
MMT:Co(Phen)$_2$	Co	1.47×10^4
MMT:Fe(Phen)$_2$	Fe	18.3×10^4

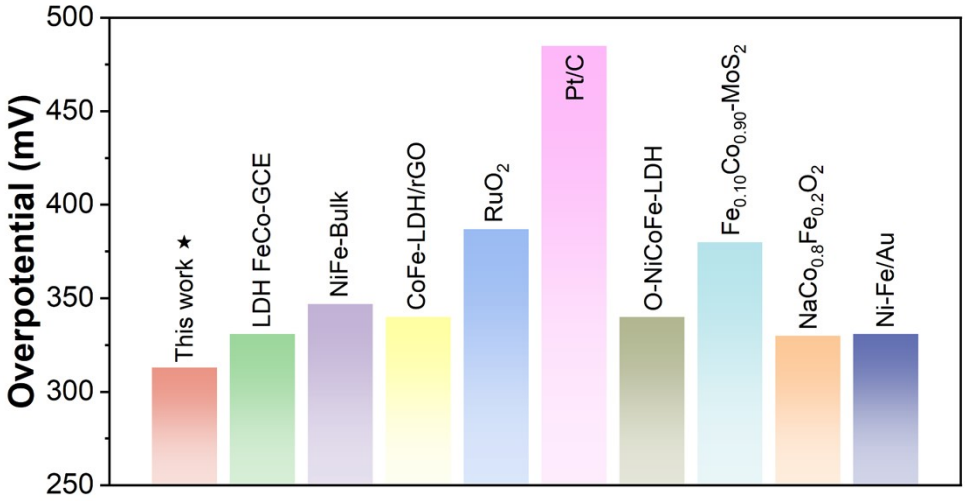

Figure S9. Comparison of η_{10} values for MMT:Co(Phen)$_2$ and other OER catalysts in 1M KOH.

Table S7. Comparative analysis of η_{10} values for various OER catalysts.

Sample	Overpotential @ 10 mA·cm^{-2}	*electrolyte*	*Ref.*
LDH FeCo-GCE	331 mV	1 M KOH	[1]
NiFe-Bulk	347 mV	1 M KOH	[2]
CoFe-LDH/rGO	340 mV	1 M KOH	[3]
RuO_2	387 mV	1 M KOH	[3]
Pt/C	485 mV	1 M KOH	[3]
O-NiCoFe-LDH	340 mV	1 M KOH	[4]
$Fe_{0.10}Co_{0.90}$-MoS_2	380 mV	1 M KOH	[5]
$NaCo_{0.8}Fe_{0.2}O_2$	330 mV	1 M KOH	[6]
Ni-Fe/Au	331 mV	1 M KOH	[7]
MMT:Co(Phen)$_2$	313 mV	1 M KOH	This work

References

1. B. Zhang, X. Zheng, O. Voznyy, R. Comin, M. Bajdich, M. García-Melchor, L. Han, J. Xu, M. Liu, L. Zheng, F. P. García de Arquer, C. T. Dinh, F. Fan, M. Yuan, E. Yassitepe, N. Chen, T. Regier, P. Liu, Y. Li, P. De Luna, A. Janmohamed, H. L. Xin, H. Yang, A. Vojvodic and E. H. Sargent, *Science*, 2016, **352**, 333-337.
2. F. Song and X. Hu, *Nat. Commun.*, 2014, **5**, 4477.
3. X. Han, C. Yu, J. Yang, C. Zhao, H. Huang, Z. Liu, P. M. Ajayan and J. Qiu, *Adv. Mater. Interfaces*, 2016, **3**, 1500782.
4. L. Qian, Z. Lu, T. Xu, X. Wu, Y. Tian, Y. Li, Z. Huo, X. Sun and X. Duan, *Adv. Energy Mater.*, 2015, **5**, 1500245.
5. K. Sathiyan, T. Mondal, P. Mukherjee, S. G. Patra, I. Pitussi, H. Kornweitz, R. Bar-Ziv and T. Zidki, *Nanoscale*, 2022, **14**, 16148-16155.
6. B. Weng, F. Xu, C. Wang, W. Meng, C. R. Grice and Y. Yan, *Energy Environ. Sci.*, 2017, **10**, 121-128.
7. X. Yu, M. Zhang, W. Yuan and G. Shi, *J. Mater. Chem. A*, 2015, **3**, 6921-6928.